INTERNATIONAL PACIFIC HALIBUT COMMISSION

**ESTABLISHED BY A CONVENTION BETWEEN
CANADA AND THE UNITED STATES OF AMERICA**

Technical Report No. 29

Estimating Sex of Pacific halibut (*Hippoglossus stenolepis*) Using Fourier Shape Analysis of Otoliths

by

Joan E. Forsberg
International Pacific Halibut Commission
and Phillip R. Neal
Department of Statistics, University of Washington

Technical Report No. 30

A Bibliography on Atlantic Halibut (*Hippoglossus hippoglossus*) and Pacific Halibut (*Hippoglossus stenolepis*) Culture, with Abstracts

compiled by

Robert R. Stickney and Damon Seawright
School of Fisheries, University of Washington

SEATTLE, WASHINGTON
1993

INTERNATIONAL PACIFIC HALIBUT COMMISSION
P.O. BOX 95009
SEATTLE, WASHINGTON 98145-2009, U.S.A.

Contents

3

Technical Report No. 29

Estimating Sex of Pacific Halibut (*Hippoglossus stenolepis*) Using Fourier Shape Analysis of Otoliths

by

Joan E. Forsberg
International Pacific Halibut Commission
and
Phillip R. Neal
Department of Statistics, University of Washington

ABSTRACT

At present, the sex ratio of the commercial halibut catch cannot be obtained easily, since the gonads are removed at sea. Halibut otoliths, which are collected by the International Pacific Halibut Commission (IPHC) for age determination, appear to have sex-related shape differences. A technique for sexing otoliths based on such shape differences would be a cost-efficient way to make this information available. In an attempt to quantify and analyze the apparent shape differences, Fourier shape descriptors are obtained from digitized otolith images. The descriptors, with and without otolith weight, are used to classify otoliths by sex. The data are divided into training and test sets of various sizes for classification analysis. Successful classification rates range between 71.4% and 73.6% for the test sets when otolith weight is included in the analysis. When the descriptors alone are used, successful classification rates are 63.9% to 65.3% for the test sets. Training set success rates are higher for males, a finding indicating somewhat higher variation in otolith shape among females. Given the results achieved in this study, otolith shape does not appear to be a reliable indicator of sex in Pacific halibut.

Estimating Sex of Pacific Halibut (*Hippoglossus stenolepis*) Using Fourier Shape Analysis of Otoliths

by

Joan E. Forsberg
International Pacific Halibut Commission
and Phillip R. Neal
Department of Statistics, University of Washington

INTRODUCTION

The International Pacific Halibut Commission (IPHC) recently observed changes in weight-at-age relationships in commercially caught Pacific halibut (*Hippoglossus stenolepis*). Because there is a significant difference in the growth rates of male and female Pacific halibut (McCaughran 1987), IPHC staff suggested that this change might be due to a shift in the sex ratio. This hypothesis cannot be tested, however, since at present, sex ratio information from the commercial catch cannot be easily obtained.

To date, there are only two ways to reliably sex halibut: examination of the external genitalia of live or undressed fish (St-Pierre 1992), or examination of the gonads. IPHC staff collect otoliths along with daily fishing records as commercially caught halibut are being unloaded at processing plants, but because halibut are dressed at sea, sexing by either method is not possible. The IPHC has investigated other methods of sexing halibut in the past; however, a method that could be applied to the commercial catch has yet to be found. Presence or absence of egg vitellin protein (found in the blood of mature females) can be used as an indicator of sex for mature individuals, but it is incapable of distinguishing between males and immature females (C. C. Schmitt, pers. comm.)[1]. Moreover, the technique was not tested with any of the body fluids or tissues that would remain in a dressed fish, and even if it was found to be successful, implementation of this technique would be quite costly if used for large-scale sampling of the commercial catch.

IPHC otolith readers, who have examined large numbers of known-sex halibut otoliths, have observed that otoliths from male and female halibut are different in appearance. The most obvious difference is size; otoliths of male halibut tend to be smaller in both length and weight, than those of females at a given age. In on-going studies at the IPHC, otolith length and weight differences have been considered for possible use in estimating sex ratios. However, there is considerable overlap in otolith size between the sexes.

In addition to the differential in otolith size, there are also subtle differences in otolith shape between the sexes. For example, male otoliths tend to be more elongate than female otoliths, whereas many female otoliths are broad at the posterior end and narrower at the anterior portion. Male otoliths tend to be thicker in relation to overall size and length than female otoliths. This difference is more pronounced in older fish, but can also be seen in otoliths from younger fish, particularly in the posterior half (Figures 1 and 2). Associated with this thickness in male otoliths is a steep slope or drop to the edge of the otolith, as opposed to the more flattened edge of female otoliths. A technique for sexing otoliths using a series of measurements that would reflect any of these morphological differences would be cost-efficient, time-saving, and objective. Otoliths are already collected for age analysis; therefore, extra data collection trips would not be necessary, nor would additional equipment be required for morphometric analysis. This paper describes a two-part study, the purpose of

---

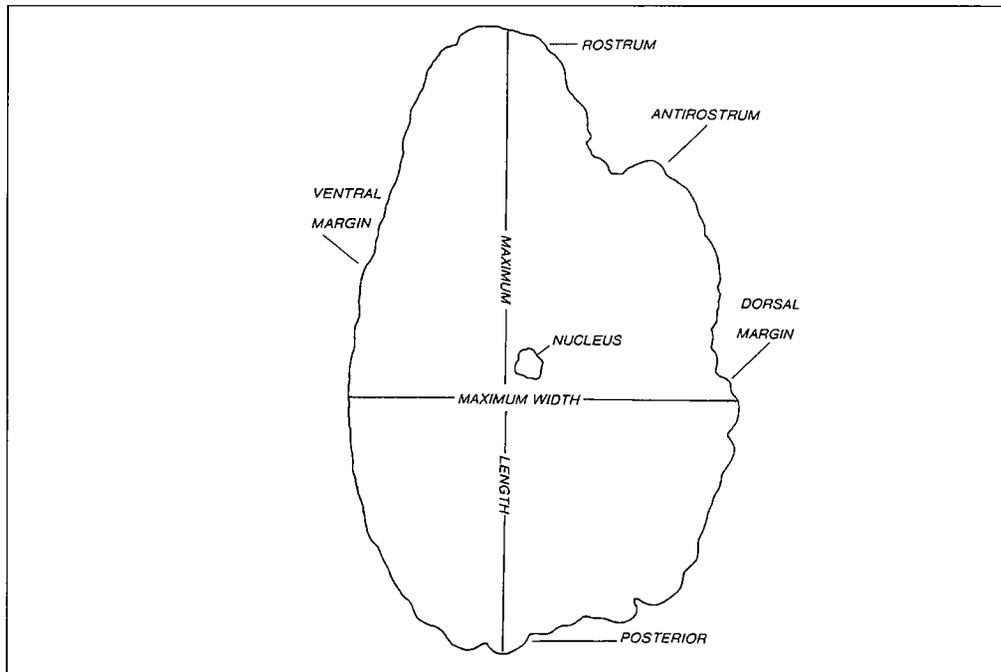[1]Schmitt, C. C. Washington Department of Fisheries, Olympia, WA.

7

Figure 1. Diagrammatic view of distal side of a left sagittal otolith of a Pacific halibut (After Härkönen, 1985).
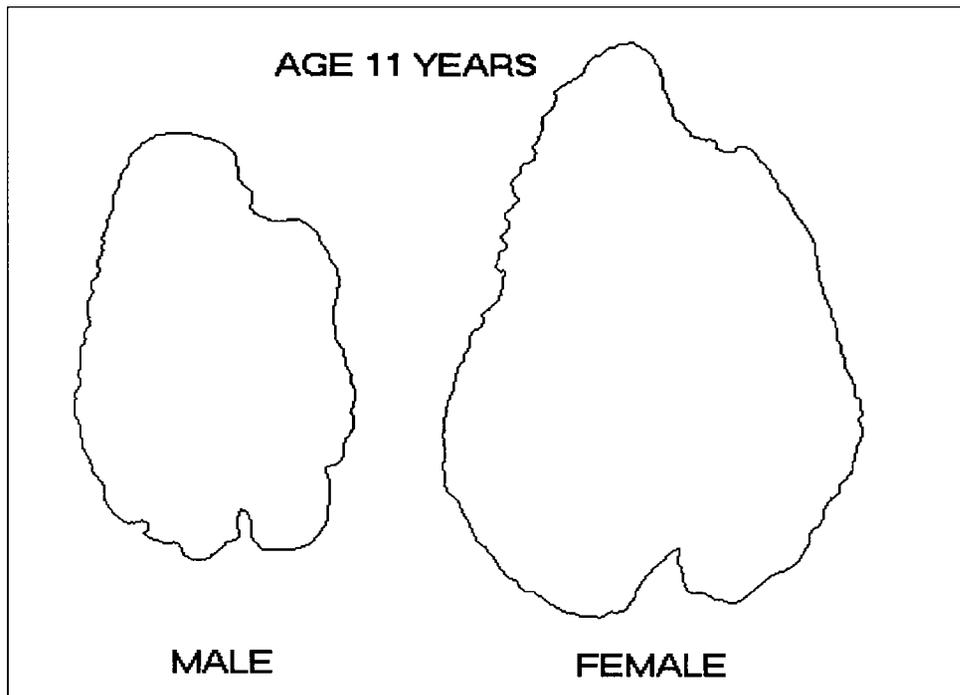

Figure 2. Comparison of male and female halibut otoliths, (digitized image outlines of two otoliths used in this study) illustrating typical size and shape differences.

which was to determine if otolith shape could be used to discriminate between male and female Pacific halibut.

Our first approach was to establish whether there is a quantifiable difference in otolith elongation between the sexes, which would be reflected in the otolith length-width ratio. This preliminary study, using measurements of otolith length and width, revealed considerable overlap between the sexes. Simple length and width measurements proved to be rather crude shape descriptors so a second approach, Fourier shape analysis, was utilized on a subset of the otolith sample. We used a subset of a single age group to eliminate possible effects of age-related shape differences. We chose 11-year-olds because they are one of the more prevalent age groups in the commercial catch.

Fourier shape analysis is a way of describing a closed 2-dimensional shape as a series of coefficients, in order to condense the data and make comparisons between shapes possible. Fourier shape analysis can be used to classify images of objects by comparing an unknown shape with reference shapes (Wallace and Wintz 1980), or to distinguish between different shape types (Bird et al. 1986, Pandolfi and Burke 1989). A closed 2-dimensional shape can be traced and the boundary points, or x,y coordinates, can be used to create a single complex function that describes the shape. An algorithm called an FFT (Fast Fourier Transform) converts the set of x,y coordinates to a set of paired coefficients called a Fourier series. Each coefficient pair is composed of a real and an imaginary part (Wallace and Wintz 1980). The paired coefficients, also called Fourier descriptors, can be compared with coefficients from other shapes.

In fisheries applications, Fourier shape analysis of scales has been employed for stock separation and identification. Success rates of classification by this method vary widely with the species used. Pontuel and Prouzet (1988) obtained success rates as high as 99.5% between two stocks of Atlantic salmon, whereas Riley and Carline (1982) achieved success rates for five western Lake Erie walleye stocks that were only slightly better than random. Fourier shape analysis has also been used to describe teleost otolith shape. Bird et al. (1986) used Fourier descriptors to establish differences in otolith shape between adult Alaskan and northwest Atlantic herring and between juvenile and adult herring otoliths within the same stock. Fourier analysis of otolith shape was also used to compare different stocks of Atlantic mackerel (Castonguay et al., 1991), and to compare populations of Pacific deep slope red snapper (Smith, 1992). Sex-related shape differences in scales or otoliths are discussed in Bird et al. (1986), Riley and Carline (1982), and Castonguay et al. (1991); however, none of these authors found sufficient sexual dimorphism in otolith or scale shape to classify successfully by sex. The goal of shape analysis of fish scales or otoliths is generally stock separation, and very little has been done using otolith morphology or shape analysis for the sole purpose of distinguishing sex.

MATERIALS AND METHODS

Otolith Sample

Six hundred left-side sagittal otoliths, composed of four age groups: 9-, 10-, 11- and 12-year-olds, were measured for maximum length and maximum width and used in the preliminary study. Within each age group, 75 otoliths each from male and female fish were examined. All otoliths were taken from fish of known sex (determined by gonad examination) caught in the central Gulf of Alaska (IPHC Regulatory Area 3A, Figure 3) during IPHC longline surveys in 1984 and 1986. We used 144 of the age-11 otoliths (74 male, 70 female) for Fourier shape analysis. All IPHC survey otoliths were aged at least twice, three times if the first and second ages disagreed. Age estimates were made by surface annuli counts. We selected otoliths that were not broken or crystallized, and for which at
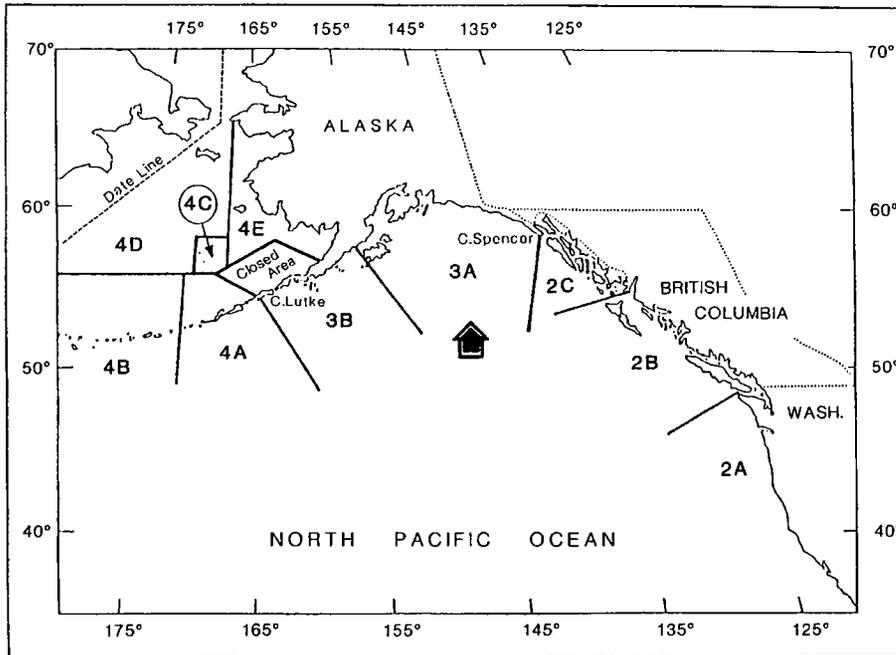
Figure 3.   **Map of Gulf of Alaska showing IPHC Regulatory Areas.**

least two of the three age determinations were the same, with the third differing by no more than one year.

Hardware and Software

The digital image analysis system consisted of a Matrox frame grabber, a MTI vidicon camera, a Wild M5a binocular dissecting microscope with a Volpi 0.5X demagnifier, and a Panasonic MT 1340 G color video monitor. Fourier shape analysis was performed using the OPRS© image analysis software from BioSonics (1987) running on a Compaq Desqpro 386 personal computer. Software used to collect length and width measurements was written by the second author.

Otolith Measurements

Otolith measurements of maximum length and maximum width were taken from digitized images at 3X magnification. The procedure for obtaining measurements was semi-automated. The only manual step was the alignment of the otolith under the microscope. Measurements were obtained using luminance values, then converted from pixel units to millimeters before analysis. Length-width ratios (maximum width ÷ maximum length) were calculated and frequencies of the ratios were plotted for males and females. Ratios were used to remove the effects of size variation. Otolith weights (measured in milligrams) and surface ages (in years) were already available.

Fourier Analysis

Fourier coefficients, or descriptors, were generated using the OPRS software (BioSonics 1987). This program traces outlines automatically by following the path of highest luminance gradient using the Roberts Edge Detector algorithm, to trace the image outline. This algorithm computes the absolute value of the difference between luminance values of neighboring pixels. The gradient of a pixel at position x,y with a luminance value of f(x,y) is defined as:

(1)   gradient = abs(f(x,y) - f(x+1,y+1)) + abs(f(x,y+1)-f(x+1,y)).

The gradient is calculated for each of the eight neighbors of the current position, and the pixel position with the largest gradient becomes the new position. The x and y coordinates of the resulting traced outline are sampled at equidistant intervals. The N sampled points are stored in vectors x(t) and y(t), where t is the sequence number of the sampled point. The Fourier descriptors of these two series, x(t) and y(t) are defined as the complex coefficients of their combined Fourier series approximation: Let these two real vectors, x(t) and y(t) of length N be combined into one complex vector z(t), with the x(t) representing the real part and the y(t) representing the imaginary part of the complex vector. This complex vector can then be approximated by a discrete, truncated Fourier series represented in complex form as:

$$(2) \qquad z(t) \approx \frac{1}{N} \sum_{n=0}^{N-1} A(n)\exp\left(\frac{-2\pi j t n}{N}\right)$$

where:

$z(t)$ = the complex vector of sampled points
N = the number of points sampled
$A(n)$ = the complex Fourier coefficients
$\exp$ = the exponential operation
j = the square root of -1
t = the index of the sampled point
n = the index of the frequency

The Fourier descriptors are then normalized for translation, size, and rotation before being used in discriminant analysis. Setting A(0) to zero translates the center point of the contour to (0,0). Size normalization is done by dividing each coefficient A(i) by | A(1) |. The first coefficient of each series corresponds to the circular component of the contour. Finally, rotation and starting point normalizations are done by converting the phases of the two coefficients of largest magnitude to zero. A(1) is the coefficient of largest magnitude. A search for A(k), the coefficient of second largest magnitude, and the resolution of ambiguity is detailed in Wallace and Wintz (1980). The whole normalization process can be described as follows:

Step 1.   Set A(0) to 0. This will center the contour around (0,0).
Step 2.   Divide all the A(i) by the modulus of A(1). This will normalize for size.
Step 3.   Find the Fourier coefficient of second largest magnitude A(k)
Step 4.   Compute u and v the phases of A(1) and A(k) respectively.
Step 5.   Apply the rotation and starting point normalizations by multiplying the A(i) coefficients by

(3)
$$\exp(\frac{j[(i-k)u+(1-i)v]}{(k-1)})$$

Step 6.   If k=2, the normalization process is complete. A(n) now contains the normalized Fourier descriptors.

Step 7.   Compute the number of possible normalizations $m(k) = |(k-1)|$.

Step 8.   For each of the possible $m[k]$ normalizations:
           a. Compute the ambiguity resolving criterion (AC):

(4)
$$AC = \sum_{i=1}^{N-1} Re\ [A(i)]\ |Re[A(i)]|$$

           where Re = the real half of the Fourier coefficients
           Save the AC as well as the A(n) for this normalization.
           b. Multiply the A(i) by

(5)
$$\exp(\frac{j(i-1)2\pi}{m[k]})$$

Step 9.   The A(n) of the normalization with the largest AC among the $m[k]$ normalizations is the set of normalized Fourier descriptors to be used.

This *Cartesian* or *complex* FFT algorithm is capable of describing both convex and concave shapes. Because some halibut otoliths have concavities in their shape outlines, we decided that the Cartesian FFT was more suitable. The algorithm more commonly used in Fourier shape analysis of scales and otoliths, the *polar* or *radial* FFT is capable of describing only convex shapes, (i.e., a shape that can be described as a single-valued function about a central point or "centroid") and generates Fourier coefficients by projecting a series of radius vectors from the shape centroid to the shape boundary. For this algorithm to accurately describe a shape, each radius must pass through a single point on the shape boundary. However, if a shape had concavities, some radii would pass through more than one point on the shape boundary, and since only the first point at which a radius intersects the outline is used in generating the Fourier series, part of the shape information will be lost. (See Figure 4).

The use of a Cartesian FFT makes it somewhat difficult to compare the results of this study on a descriptor by descriptor basis with those of other workers for the following reasons: Radial FFTs, such as those used by Bird et al. (1986) and Pandolfi and Burke (1989) output the descriptors such that the low-end FDs (Fourier Descriptors) are those that control gross shape, while the high-end FDs modify fine surface perturbations. Also, since the Fourier series generated by a radial FFT is symmetric about its midpoint (i.e., FDs [1 to $N/2$] are the mirror image of FDs [N to $\{N/2+1\}$]), only the first $N/2$ descriptor pairs are analyzed. On the other hand, the Fourier series generated by a complex FFT is not symmetric about its midpoint. The FDs generated by the algorithm used in this study are output such that gross shape descriptors are located in both ends of the FD vector, and descriptors modifying the finer perturbations comprise the middle FDs. Also, the number of FDs generated and/or used for analysis varies between studies, and this variation makes comparisons between specific pairs difficult.

As in the collection of length and width measurements, the procedure for obtaining Fourier coefficients was also semi-automated in that the only manual step was marking the

starting point on the image for the tracing routine. For each otolith image, 128 descriptor pairs were obtained. The resulting data set was reduced prior to classification analysis, and the coefficient pairs containing the most information (based on the coefficient means) were used in classification analysis. Twenty coefficient pairs were selected for classification analysis. Chosen were pairs 3 through 12, and pairs 119 through 127, plus 128_R (subscript "R" refers to the real portion of the descriptor pair). The first 2 coefficient pairs, as well as the imaginary half of the 128th pair, were identical for all images as a result of the size normalization procedure and were therefore excluded from the analysis.

Classification Analysis

A classification vector was constructed consisting of the 20 real and 19 imaginary Fourier coefficients, with and without the corresponding otolith weights. This classification vector was then used as input for Linear Discriminant Function Analysis (LDFA). LDFAs were performed using the DISCRIMINANT program of SPSS-X (SPSS 1988).
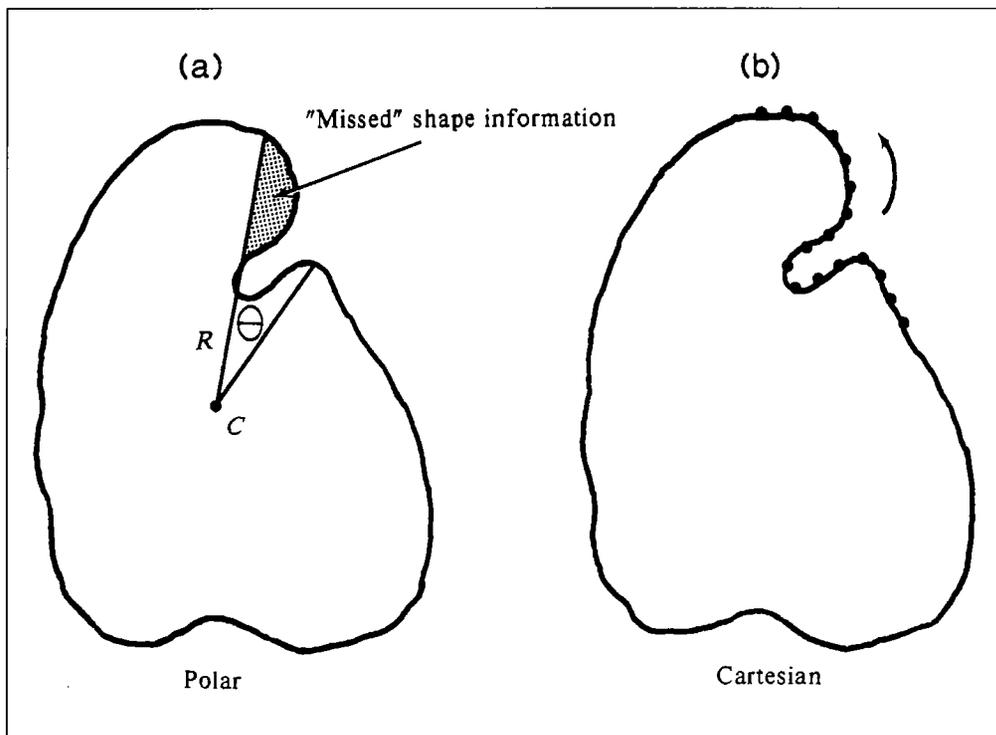
Figure 4.   Example of a concavity in a halibut otolith outline. The shape is more accurately described by the Cartesian method (b) than by the polar method (a). In (a), the radius intersects the outline at two points; however, only the first point is used in generating the Fourier series.
Figure 4a. FFT generated by sampling at a constant angle theta (θ) from the centroid (C), the first point on the outline intersected by each radius (R).
Figure 4b. FFT generated by by sampling equidistant points along the shape outline.

13

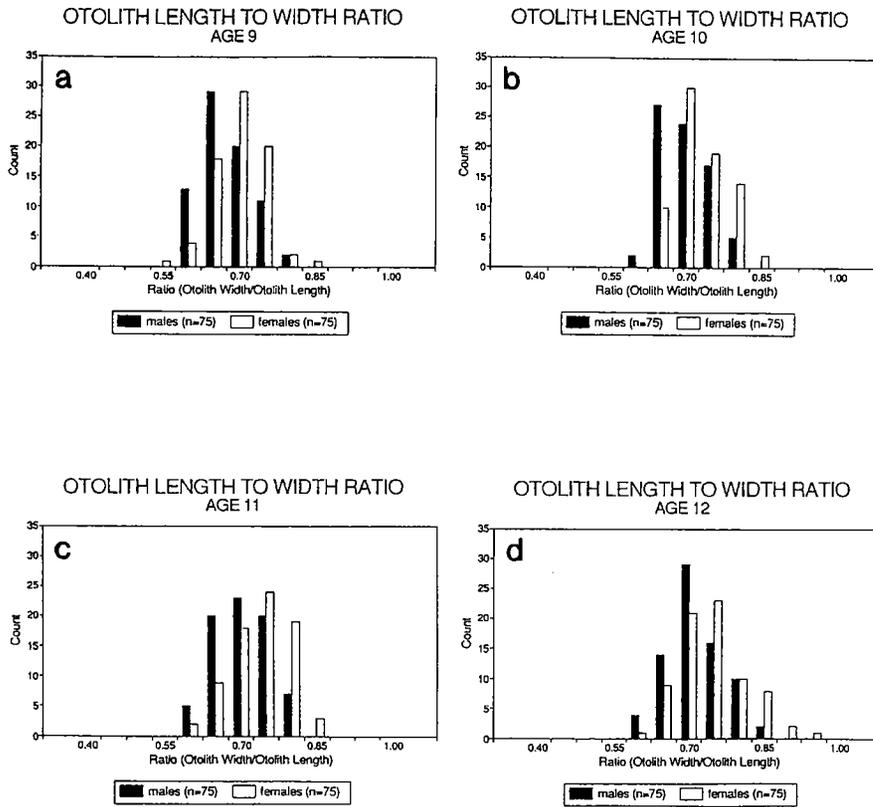**Figure 5.** Frequencies of male and female otolith length-to-width ratios (Ages 9 to 12 Years; a through d, respectively.)

Table 1. Mean otolith length-width ratios.

SEX	AGE 9	AGE 10	AGE 11	AGE 12
Male	0.6529±0.0477	0.6699±0.0482	0.6798±0.0519	0.6875±0.0552
Female	0.6756±0.0485	0.7033±0.0501	0.7130±0.0566	0.7208±0.0664

RESULTS

Length-Width Ratios

Mean length-width ratios increased slightly with age for both sexes. Male otoliths of all age groups had lower mean length-width ratios. In other words, otolith width is slightly less in proportion to otolith length for males than for females (Figure 5). Mean otolith length-width ratios for the four age groups are listed in Table 1.

Table 2.   **Discriminant analysis results: Rates of successful classification of sex.**

WITH OTOLITH WEIGHT	MALE	FEMALE	TOTAL
66% Training 33% Test	89.8% (n=49) 72.0% (n=25)	82.6% (n=46) 70.8% (n=24)	86.3% (n=95) 71.4% (n=49)
50% Training 50% Test	91.9% (n=37) 75.7% (n=37)	82.9% (n=35) 71.4% (n=35)	87.5% (n=72) 73.6% (n=72)
WITHOUT OTOLITH WEIGHT			
66% Training 33% Test	87.8% (n=49) 60.0% (n=25)	84.8% (n=46) 70.8% (n=24)	86.3% (n=95) 65.3% (n=49)
50% Training 50% Test	97.3% (n=37) 59.5% (n=37)	85.7% (n=35) 68.6% (n=35)	91.7% (n=72) 63.9% (n=72)

Classification Analysis

The software used to perform LDFAs on the data set of Fourier descriptors randomly split the data into training and test sets of varying proportions. Otolith weight was included as a parameter in half of the LDFAs, for which training set sizes were 66% and 50% of the entire data set. Parameters for the other LDFAs consisted only of the Fourier descriptors, and training set sizes were also 66% and 50% of the entire data set. Classification success rates are listed in Table 2.

LDFAs Using Descriptors and Otolith Weight

Total successful classification rates increased as training set size decreased for the training sets, ranging between 86.3% and 87.5%. The difference between male and female classification success rates also increased as training set size decreased for these LDFAs. Successful classification rates for females were lower than those for males in both trials. Success rates were 89.8% and 91.9% for males and 82.6% and 82.9% for females. Success rates for test sets were about 10% lower than those of the training sets, and again, successful classification increased with decreased training set size. The difference between male and female success rates was somewhat less for the test sets.

LDFAs Using Descriptors Only

Again, total successful classification rates increased as training set size decreased. Male classification success rates were again higher than female success rates for the two training sets. As with the LDFAs using descriptors plus otolith weight, test set scores were lower than those of training sets. In contrast to the success rates for training sets, success rates for test sets decreased as training set size decreased. Total successful classification rates were 65.3% for the 33% test set and 63.9% for the 50% test set. Classification success rates were higher for females in the test sets.

Several discriminating parameters appeared in the discriminant functions of all

Table 3. Rankings of parameters used in discriminant functions. (Subscripts "R" and "I" refer to real and imaginary)

TRAINING SET SIZE (% OF WHOLE DATA SET)			
WITH OTOLITH WEIGHT		WITHOUT OTOLITH WEIGHT	
50%	66%	50%	66%
Weight	Weight	FD 121_I	FD 121_I
FD 125_R	FD 125_R	FD 125_R	FD 125_R
FD 121_I	FD 127_I	FD 127_I	FD 127_I
FD 127_I	FD 121_I	FD 121_R	FD 127_R
FD 128_R	FD 128_R	FD 128_R	FD 121_R
FD 124_I	FD 121_R	FD 3_I	FD 128_R
FD 12_I	FD 124_I	FD 5_I	FD 6_R
FD 123_R	FD 125_I	FD 12_I	FD 8_I
FD 122_R	FD 120_I	FD 124_I	FD 119_I
	FD 122_R	FD 125_I	FD 122_R
	FD 119_I	FD 122_R	FD 125_I
	FD 6_R	FD 119_I	FD 120_I
	FD 126_R	FD 122_I	FD 126_I
	FD 11_I	FD 12_R	FD 3_I
	FD 3_I		
	FD 119_R		

Table 4. Table of means of common discriminating parameters (from whole data set).

PARAMETER	MALE MEAN (n=74)	FEMALE MEAN (n=70)
Otolith Weight (mg)	230.51	301.59
FD 121_R	0.00213	0.00030
FD 121_I	-0.00221	0.00056
FD 125_R	-0.01491	-0.01127
FD 127_I	-0.00259	0.00336
FD 128_R	-0.17725	-0.16585

LDFAs. These were Fourier descriptors (FDs) 125_R, 127_I, 121_I, and 128_R. Subscripts "R" and "I" refer to real and imaginary, respectively. Otolith weight was also common to the LDFAs for which otolith weight was a parameter. In the LDFAs using descriptors only, FD 121_R also appeared in the discriminant functions of the training sets. Size of the discriminant function varies between the LDFAs of different size training sets, as does the order of importance of some of the common discriminating parameters within the functions (see Table 3). For each of the real coefficients that were discriminating parameters, the male and female means were both either positive or negative. On the other hand, for each of the common imaginary coefficients, the male means were negative and the female means were positive. The means of the common discriminating parameters are listed in Table 4.
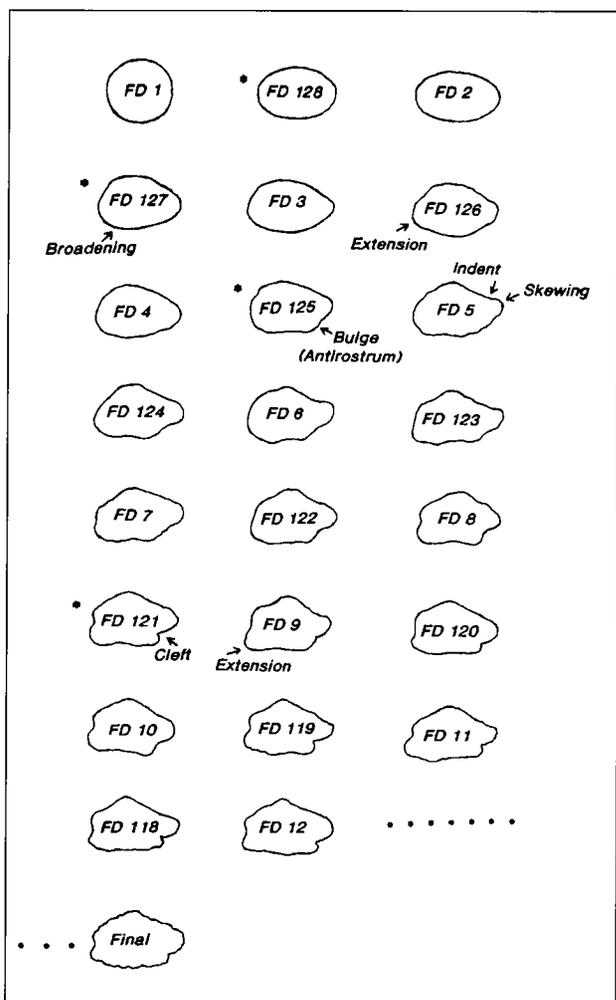
Figure 6. Stages of reconstruction of an otolith shape. (Shape outlines were traced onto paper from the monitor screen) Progression of reconstruction is stepwise from left to right, top to bottom. Each shape outline represents the summation of previous FDs up to and including the FDs inside the outline. (See RESULTS section for explanation of arrows and accompanying comments). Asterisks indicate FDs that were common discriminating parameters.

A program was used to reconstruct an otolith from its descriptors in order to evaluate the contributions of the various descriptors to overall shape (Figure 6). Descriptor pairs were incorporated into a reverse FFT one pair at a time. Each time another pair was added, the shape, resulting from the summation of the descriptor pairs added to that point, was drawn to the monitor screen. Pairs were added alternately from the two ends of the descriptor vector (i.e., pair 1, then pair 1+pair 128, then pair 1+pair 128+pair 2, etc.). Both the real and imaginary portions of each descriptor pair were used in the reconstruction. The following are descriptions of the apparent effects on shape of the Fourier descriptors used in classification analysis as observed in otolith shape reconstruction. The contribution of FD 1 is circularity, whereas FDs 128 and 2 cause elongation of the shape. When FD 127 is included, a broadening of the posterior half of the otolith results. FD 3 appears to have a narrowing effect at the anterior end, and when FD 126 is added, there is extension of the dorsal posterior edge. With the addition of FD 125, a bulge forms at the site of the antirostrum. When FD 5 is included, there is an apparent indentation of the ventral edge of the rostrum, creating a hump in the middle of the ventral margin, and the rostrum is skewed in the ventral direction. With the addition of the next few pairs, an indentation appears in the middle of the dorsal margin. Also, there is fluctuation in the shape of the posterior edge, with

alternating extension and rounding of the dorsal process. Low end descriptors seem to induce rounding, while high end descriptors influence angularity. By the time FD 121 is added, a cleft has appeared between the rostrum and antirostrum. With the inclusion of FDs 9 to 12 and 120 to 118, the dorsal and ventral processes on the posterior edge become more defined, as does the cleft between the rostrum and antirostrum. Gross shape is more or less complete at the addition of FD 12. FDs between 13 and 117 add fine bumps and surface sculpture to otolith shape.

DISCUSSION

Length-Width Ratios

Although male otoliths are slightly narrower on average than female otoliths, there is insufficient separation of length-width ratio frequency distributions for length-width ratios to be useful in classifying otoliths by sex. However, we thought that if there were shape differences apparent to the naked eye, there should be some way to quantify these differences, and that perhaps the length and width measurements simply failed to capture that information. Rather than increase the number of distance measurements, we decided to use Fourier shape analysis, in the hope that this method would detect sex-related shape differences with greater discriminatory power. Smith (1992) found that cluster analysis using Fourier shape descriptors of Pacific deep red snapper otoliths produced more discrete regional groupings than ratios of linear measurements of the same otoliths. Halibut otoliths can be correctly classified by sex 70% to 75% of the time by IPHC age readers simply by examining the otoliths visually. It is probable that the correctly classified otoliths represent the extreme ends of the shape "spectrum" (i.e., narrow, thick male otoliths and triangular-shaped, flat female otoliths,) while the misclassified otoliths represent the overlapping portions of the shape spectrum. Another factor in this ability can be attributed to the age of the otoliths, since shape differences and other characters that differ with sex, such as annulus spacing and otolith thickness, are more evident in older fish, especially those aged 15 years and older.

Classification Analysis

Overlap between the sexes is found with the Fourier descriptors, although to a lesser extent than with the length-width ratios. The purpose of using different sizes of training and test sets is to test robustness of the discriminant function to the data. Some of the same parameters show up consistently, indicating classification results and parameters chosen as discriminators are not random, and also implying that there is some sexual dimorphism in otolith shape. However, the seemingly sporadic inclusion of descriptors not common to all LDFAs and the shifting order of importance of the common descriptors in the discriminant functions indicate a certain amount of "noise." This noise is caused by variability and overlap of descriptor means; which could be due to true variation in otolith shape within each sex in this age group, or due to sex or age being incorrectly assigned to one or more otoliths in the sample, or an artifact of the data collection software.

Because the rates of successful classification are lower for females in the training sets, it is possible that female otoliths are more variable in shape than male otoliths. Results of visual examination confirm this conclusion. When otolith readers estimate sex based on visual appearance of otoliths, females are wrongly classified more often than males and appear to be more variable in shape to the naked eye. While total successful classification rates are similar for training set size for LDFAs with and without otolith weight, total success rates of test sets for LDFAs without otolith weight are much lower than those of test sets for

which otolith weight is included. These findings indicate that otolith weight is a more powerful discriminator and has less variation than any of the discriminating shape descriptors. However, test set scores are almost the same for females with or without otolith weight. These results suggest that otolith weight is more important as a discriminator in males, and less important and more variable in females. The observed increase in classification success for both training and test sets as training set size decreased is more difficult to explain and is quite likely an artifact due to the small sample size and large number of parameters.

Fourier Shape Descriptors

Significant or discriminating FDs found in this study cannot be easily compared with other researchers' findings, for reasons outlined in the methods section. Methods of analysis of Fourier shape data vary considerably, as well. Some methods use the power spectrum of the descriptor series (the square root of the sum of the squares of the real and imaginary component of each pair). However, sign information is lost when this method is used. Many researchers analyze only the real component of the coefficient pairs, whereas we analyzed both the real and imaginary portions of the pairs. With a modification to the program used to reconstruct otolith shape, it was possible to separate the components of a given pair, so we were thus able to examine the independent effects of the real and imaginary components on a simplified shape (Figure 7). When real descriptors alone are used in the image reconstruction, the image is symmetric about its length axis (Figure 7a). On the other hand, imaginary descriptors introduce asymmetry. The effect of imaginary FD sign is illustrated in Figures 7b and 7c. The image constructed only of real FDs 1_R, 128_R, 2_R and
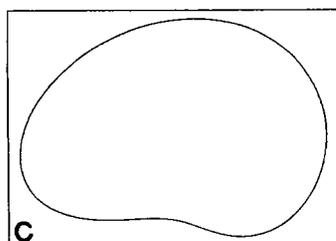
Figure 7.
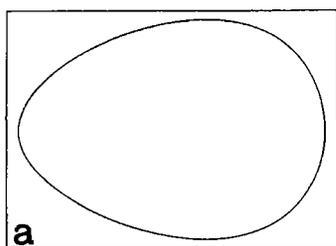
7a. **Partial otolith reconstruction using only real coefficients. (Included are: FDs 1_R, 2_R, 128_R AND 127_R).**
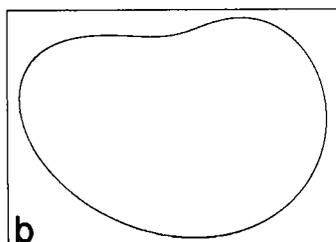
7b. **Shape (a) with the addition of FD 2_I of positive value (0.3). Results in asymmetric skewing of anterior end of otolith image.**

7c. **Sign of the imaginary coefficient reversed (FD 2_I = -0.3). Results in mirror image of shape (b).**

19

127_R, (Figure 7a,) is skewed asymmetrically by the addition of a positive imaginary FD (FD $2_I = 0.3$) in Figure 7b. When the sign of the imaginary FD is reversed (FD $2_I = -0.3$), in Fig. 7c, the image is skewed in the opposite direction so that it becomes a mirror image of that of Figure 7b. It is possible that sign change may have some sort of effect on an actual otolith outline. Given these observations and the fact that the means of the imaginary descriptors that were discrin.inating parameters were of opposite sign for males and females, we think that the inclusion of the imaginary FDs in the LDFAs is appropriate in this study. Although it is rather easy to show the effect of imaginary descriptors and sign change on a simplified shape using an exaggerated imaginary FD value, it is much more difficult to observe changes to actual otolith shapes by switching the signs of the discriminating imaginary FDs. Values of the discriminating descriptors are small, and true otolith shapes are more complicated than the simplified image of Figure 7, so small changes, such as sign change of a small coefficient value, may be masked by interactions with other shape descriptors. It is difficult to associate the exact degree of physical shape change with a specific descriptor value, as discussed by Pontuel and Prouzet (1988). However, these authors also pointed out that the ability to interpret and quantify the exact effect on shape of a given descriptor value is not of vital importance if the goal is to find descriptors with sufficient discriminatory power to allow separation and classification of groups.

One of the sex-related shape differences that was used in the discriminant functions to classify sex was elongation (FD 128). This finding is not surprising, since greater elongation of otolith shape in males is one of the features considered when humans estimate or "guess" sex of otoliths by visual examination. Another shape feature apparently used for discrimination is the breadth of the posterior half of the otolith (FD 127), again a feature used in "visual" sex estimation. There also appear to be sex-related differences with discriminatory power in the location of the antirostrum (FD 125) and in shape or position of the cleft between the rostrum and antirostrum (FD 121). The latter difference could be in relative widths or lengths of the rostrum and antirostrum, or in the angle of the cleft, as the dorsal side of the rostrum in females usually slopes at an angle to the cleft, whereas in males, the dorsal side of the rostrum often drops straight down, parallel to the length axis.

CONCLUSION

Although the Fourier descriptors of otolith shape used in this study do supply some sexual dimorphism information, the levels of classification success achieved with this information are not much better than those obtained using otolith weight and length. Given these results, we chose not to expand this pilot study sample to include age groups other than 11-year-olds. Of course, if the results had been more promising, otoliths of all age groups and from different areas would have been added to the study.

Other features that appear to differ with sex, such as otolith thickness, interannular spacing (Neal and Forsberg Unpub.)[2] or even different methods of shape analysis may yield better success rates in classification analysis for future study.

---

[2]Neal, P.R. and J.E. Forsberg. Unpub. A comparison of classifier systems for automated aging of halibut otoliths. Int. Pac. Halibut Comm. Report of Assessment and Research Activities 1991: 283 - 286.

ACKNOWLEDGEMENTS

LITERATURE CITED

BioSonics, Inc. 1987. Optical Pattern Recognition System. Data Acquisition Program Manual. Version 1.08. BioSonics Inc., Seattle, WA: 112 p.

Bird, J. L., D.T. Eppler, and D. M. Checkley, Jr. 1986. Comparisons of herring otoliths using Fourier series shape analysis. Can. J. Fish. Aquat. Sci. 43: 1228-1234.

Castonguay, M., P. Simard, and P. Gagnon. 1991. Usefulness of Fourier analysis of otolith shape for Atlantic mackerel (*Scomber scombrus*) stock discrimination. Can. J. Fish. Aquat. Sci. 48: 296-302.

Härkönen, T. 1986. Guide to the otoliths of the bony fishes of the northeast Atlantic. Danbiu ApS, Biological consultants, Hellerup, Denmark: 256 p.

McCaughran, D. A. 1987. Growth in length of Pacific Halibut, p. 507-515. *In*: R. C. Summerfelt and G. E. Hall [ed] The Age and Growth of Fish. Iowa State University Press, Ames, Iowa.

Pandolfi, J. M. and C. D. Burke. 1989. Shape analysis of two sympatric coral species: Implications for taxonomy and evolution. Lethaia 22: 183-193.

Pontuel, H. de and P. Prouzet. 1988. Numerical analysis of scale morphology to discriminate between Atlantic salmon stocks. Aquat. Living Resour. 1: 17-27.

Riley, L. M. and R. F. Carline. 1982. Evaluation of scale shape for the identification of walleye stocks from western Lake Erie. Transact. Amer. Fish. Soc. 111: 736-741.

Smith M. K. 1992. Regional differences in otolith morphology of the deep slope red snapper (*Etelis carbunculus*). Can. J. Fish. Aquat. Sci. 49: 795-804.

SPSS Inc. 1988. SPSS-X user's guide, 3rd edition. SPSS Inc., Chicago, IL: 1072 p.

St-Pierre, G. 1992. Visual determination of sex in live Pacific halibut. ICES J. mar. Sci. 49: 373-376.

Wallace, T. P. and P. A. Wintz 1980. An efficient three-dimensional aircraft recognition algorithm using normalized Fourier descriptors. Computer Graphics and Image Processing 13: 99-126.